Fibers and Polymers 2018, Vol.19, No.7, 1420-1427
DOI 10.1007/s12221-018-1134-0

ISSN 1229-9197 (print version)
ISSN 1875-0052 (electronic version)

Coloration and Decoloration of Textiles Using a TiO_2 Composite Pigment

Xiao Wang[1]*, Yunzhe Xie[1], Cheng Huang[2]*, Yongzhu Cui[1], Lihua Lyu[1], Yuping Zhao[1], and Ju Wei[1]

[1]*School of Textile and Material Engineering, Dalian Polytechnic University, Dalian 116034, China*
[2]*College of Chemistry, Chemical Engineering and Biotechnology, Donghua University, Shanghai 201620, China*
(Received November 21, 2016; Revised February 3, 2018; Accepted April 30, 2018)

Abstract: A colorable pigment was prepared by dye adsorption onto titanium dioxide and subsequent silane coating. The effects of pH value, dye concentration, and adsorption times on dye adsorption were discussed. Large adsorption capacity of an anionic dye was obtained at pH value of 2 and the adsorption process was well described by the Langmuir isotherm model. Good dyeability and color fastness of pigment dyed fabric were achieved in the normal life cycle under sunlight. The decoloration of pigment was realized through photocatalytic degradation of dye molecules by titanium dioxide under ultraviolet irradiation when reusing the pigment dyed textiles after disposal. The new absorption peaks in the FTIR spectrum at 2924.95 cm^{-1}, 1714.91 cm^{-1}, 1461.17 cm^{-1}, and 1289 cm^{-1} verified silane modification. Silane modification improved fixation of dyes onto the pigment and immobilization of pigments onto substrates. The close attachment of silane coating layer to titanium dioxide was conducive to photodegradation of dye molecules in the pigment.

Keywords: Pigment, TiO_2, Coloration, Silane modification, Photocatalytic degradation

Introduction

Large quantities of dyes, salts, and other additives are used in common coloration process of substrates such as textiles, leather, and so on. Due to low utilization ratio of dyes during dyeing process, large amount of dye wastewater containing substantial dye compounds has been discharged from coloration process, leading to a serious pollution problem. Moreover, colored fabrics are difficult to be decolorized when recycling. Advanced oxidation processes involving TiO_2/UV system has potentially been used in decoloration of dye effluents, based on reactive species such as hydroxyl radicals (•OH) generated from TiO_2 after absorbing ultraviolet light, which oxidize organic pollutants [1-3]. TiO_2 is widely applied because of not only high photocatalytic property, but also non-toxicity and chemical stability. Intensive research has been conducted on TiO_2 with various forms and structures for use in photocatalytic degradation of dye molecules in aqueous dye solution. Nevertheless, most of the studies focused on improvement of photocatalytic activities of TiO_2 such as dye sensitization, surface modification, doping, and optimizing nanostructure [4-11]. Hybrid TiO_2 pigments have rarely been reported. There were several reports that TiO_2 hybrid pigments were prepared by phthalocyanine dye or other oxide metal material enwrapping for infrared reflective property and food dye adsorption for a pharmaceutical purpose [12].

Silane coupling agents are often employed in surface modification of inorganic particles to improve interfacial compatibility. The modification of pristine TiO_2 with silane coupling agents was performed in an attempt to improve interfacial adhesion, to control charges, to enhance chemical reactivity, and to change dispersibility [13-16]. Moreover, it has been reported that silane coupling agents were used for fixation and improving light fastness of different dyes [17,18].

This paper aimed to prepare a colorable/discolorable TiO_2 composite pigment imparting color to textiles at the coloration stage, and removing color via photodegrading dye molecules by TiO_2 under UV light with short wavelength at the disposal stage for convenient recycling of textiles. The color of pigment was derived from dye molecules adsorbed onto nanosize TiO_2 particles with large surface area. Silane modification was expected to aid fixation of adsorbed dyes onto TiO_2 in the pigment and immobilization of pigment onto substrates. UV resistant agent was involved to keep dye molecules from being photodegraded by UV light in the sunshine in textile usage.

Experimental

Materials

Materials used in this study are as follows; TiO_2 particles (P25, diameter of about 21 nm, Degussa Co., Germany). Cibacron Blue FN-R (anionic dye, C.I. Reactive Blue 235, Ciba Specialty Chemicals Co., Switzerland). Hydrochloric acid (Tianjin Tianhe Chemical Reagents Factory, China, chemical pure). Sodium silicate (Tianjin Kermel Chemical Reagents Development Centre, China, chemical pure). 3-Methacryloxypropyltrimethoxy silane (KH570, J&K Scientific Co., Ltd., China, chemical pure, CH_2=C(CH_3)$COOCH_2CH_2CH_2Si(OCH_3)_3$, CAS:2530-85-0). Ethanol (Liaoning Xinxing Reagents Co., China, chemical pure). Dye-fixing agent AD300 (CHT company, chemical pure). Acetic acid (Tianjin Kermel Chemical Reagents Development Centre, China, chemical pure). Clariant C UV absorbing agent (Clariant corporation, chemical pure).

*Corresponding author: wangxiao@dlpu.edu.cn
*Corresponding author: huangch1988@yeah.net

Table 1. Operating parameters of dye adsorption onto TiO_2 particles

Sample	TiO_2 (g)	Water (m*l*)	pH value	Dye concentration (g/*l*)	Volume of dye solution (m*l*)	Stirring time (min)
The 1st adsorption	0.8	25	2-10	1.6	25	30
The 2nd adsorption	0.8	25	2-10	1.6	25	30
The 3rd adsorption	0.8	25	2-10	1.6	25	30
The 4th adsorption	0.8	25	2-10	1.6	25	30
Influence of concentration on dye adsorption (1st adsorption)	0.32	10	2	0.4-4.0	10	30
Influence of concentration on dye adsorption (2nd adsorption)	0.32	10	2	0.4-4.0	10	30

Dye Adsorption onto TiO_2

TiO_2 aqueous suspension was ultrasonically prepared using an FS-600 Ultrasonic Processor (Shanghai Shengxi Ultrasonic Instrument Co., Ltd., China) using hydrochloric acid and sodium silicate to adjust the pH value. Dye solution was subsequently added. Since dye adsorption occurred rapidly, dye adsorption amount varied with adsorption time scarcely. Adsorption time of 30 min at ambient temperature was selected to ensure the stable operation. The effects of pH value, adsorption times and dye concentration were discussed. The detailed operating conditions were listed in Table 1.

The dye concentration was measured using a UV-8000 UV/visible spectrophotometer (Shanghai Metash Instrument Co., Ltd., China). The amount of dye adsorbed on fiber was determined according to the difference of concentrations in a dye liquor before and after adsorption.

The adsorption isotherm was correlated with the Langmuir and Freundlich models [19-21].

The Langmuir equation was

$$\frac{C_e}{q_e} = \frac{C_e}{q_m} + \frac{1}{K_L q_m} \quad (1)$$

where q_e is the amount of dye adsorbed onto TiO_2 particles at equilibrium (mg/g), C_e is the dye concentration at equilibrium in the dye aqueous solution (mg/*l*), q_m is the saturated adsorption amount of monolayer, and K_L is the Langmuir adsorption constant.

The Langmuir equation can be transformed into Scatchard model. It was

$$\frac{q_e}{C_e} = K_L q_m - K_L q_e \quad (2)$$

The Freundlich equation was

$$\log q_e = \log K_F + (1/n)\log q_e \quad (3)$$

where q_e is the adsorption amount at adsorption equilibrium (mg/g), C_e is the concentration at equilibrium (mg/*l*), K_F and $1/n$ are Freundlich constants.

Preparation of Unmodified and Modified Pigments

For preparation of unmodified and silane modified pigments, dye adsorption of TiO_2 particles was conducted in dye aqueous solution of 1 g/*l* and 0.6 g/*l* successively, introducing a large amount of dye molecules onto the surface of TiO_2 to impart a deep color of pigment. Sequentially 0.32 g pigment was ultrasonically dispersed in solution containing 0.2 g silane coupling agent dissolved in 9 m*l* ethanol and 1 m*l* deionized water. The silane was hydrolyzed at pH=4 for 30 min before adding the pigment. The unmodified pigment was made without addition of silane coupling agent in this step. Afterwards the suspension sample was treated at 65 °C for 3 h for condensation of silane polymer. The pigments were washed via suction filtration with ethanol and distilled water several times and then dried in an oven at 80 °C.

To learn dye fixation in the pigment, 1.6 g unmodified or modified pigments were washed twice to calculate dye desorption ratio. The two pigments were firstly ultrasonically dispersed for 6 min in the liquid containing 10 m*l* ethanol and 10 m*l* deionized water. After suction filtration, the pigments were then ultrasonically dispersed for 1 min in 10 m*l* deionized water. Measuring the residual dye concentration, the desorption ratio was calculated by percentage of amount of desorbed dye in initial amount of dye adsorbed onto TiO_2.

Characterization of Pigments

The particle size and zeta potential analyzer (DelsaNano C, Beckman Coulter Inc., USA) was employed for measurement of zeta potential of TiO_2 particles under different pH conditions adjusted by 1 mol/*l* HCl and 0.25 mol/*l* Na_2SiO_3 aqueous solutions. The TiO_2 particles or adsorbed TiO_2 with dyes were ultrasonically dispersed in distilled water, after which pH value was adjusted. Some dye molecules desorbed from TiO_2 into water when measuring zeta potential. The Fourier transform infrared (FTIR) spectra of pigments grinded with KBr pellets were measured using Spectrum One-B instrument (PE Co., USA). The chromatic aberration (ΔE^*) of pigments was examined by an SP64

spectrophotometer (X-Rite Co., America) directly. The thickness of dye adsorption layer and silane polymer layer in pigments was observed via a transmission electron microscope (TEM, JEOL JEM-2100, Japan).

Decoloration of Pigments

3.2 g unmodified or modified pigments were ultrasonically dispersed in 34 m*l* deionized water for 20 min. Then the two pigments were irradiated under two UV lights (365 nm UV light, 185 nm, and 254 nm UV light) with the addition of water for a certain period (0.3 h, 0.7 h, 1 h, 1.3 h, 2 h, 5 h, and 8 h) using a BZZ20G-T UV-irradiation equipment (185 & 254 nm, 100 W) and a GZJ100F-XH-2 UV-irradiation equipment (365 nm, 100 W) (Shanghai Guoda UV Equipment Co., Ltd., China). The pigments were collected by suction filtration and oven drying.

Coloration and Decoloration of Cotton Fabrics with Pigments

The pigment suspension with the concentration of 0.5 wt% and bath ratio of 1:30 (mass of pigment/volume of water) was dispersed by an FS-600 ultrasonic processing equipment for 10 min. Then dye-fixation agent AD300 of 1 g/*l* was added for immobilization of pigments onto cotton fabrics. After shaking in water bath at 40 °C for 20 min, cotton fabrics were immersed, padded, and dried. Subsequently, UV resistant treatment was performed under the conditions of bath ratio of 1:40, temperature of 25 °C, Clariant C UV absorbing agent concentration of 1.4 wt%, immersion time of 40 min.

The chromatic aberration (ΔE^*) and color depth (K/S) of colored fabrics was measured by an SP64 spectrophotometer. The color fastness to rubbing was tested according to ISO standard 105-X12:1993, and the grade of dry and wet rubbing fastness were examined with gray sample card for assessing staining (ISO 105/A03-1993). The pigment dyed cotton fabrics were irradiated under two UV lights (365 nm UV light, 185 nm and 254 nm UV light) with the addition of water for a certain period (1 min, 3 min, 5 min, 7 min, 15 min, 20 min, 30 min, 45 min, 60 min, and 120 min) to observe the variation of ΔE^*.

Results and Discussion

Effects of pH Value and Adsorption Times on Dye Adsorption onto TiO_2

The influence of pH value and adsorption times on dye adsorption was seen in Figure 1. The zeta potential at various pH levels was shown in Figure 2. Under acidic conditions, the change of adsorption amount was in accordance with pH alteration in the first adsorption process. Because of surface protonation and large surface area of TiO_2 nanoparticles, the anionic dye molecules were adsorbed onto TiO_2 nanoparticles instantly via electrostatic and van der Waals interaction. Little variation in adsorption was found above the pH value of 6. The surface protonation of nanoparticles accounting for positive zeta potential under acidic conditions was conducive to adsorption of the anionic dye. Under neutral and alkaline conditions of the first adsorption process, less amount of dye molecules was adsorbed via van der Waals under the driving force from dye concentration difference, independent of pH value.

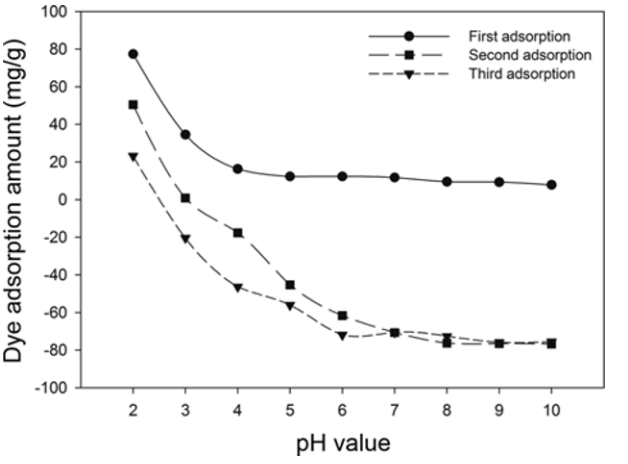

Figure 1. The influence of pH value on dye adsorption.

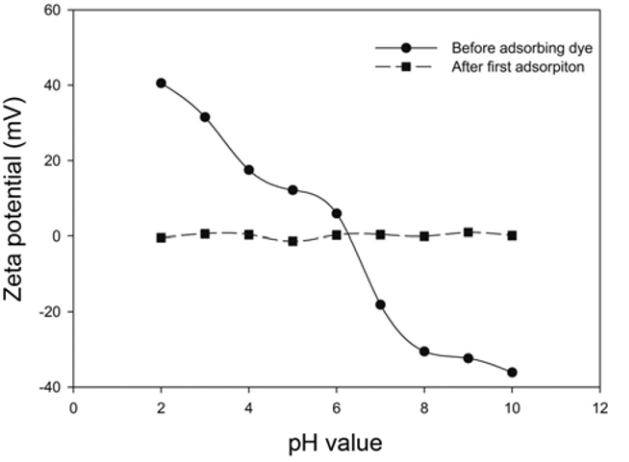

Figure 2. Zeta potential of TiO_2 particles before and after dye adsorption at different pH value.

Only at pH value of 2, dye adsorption occurred in the repeated adsorption process until the third adsorption. The negative values of dye adsorption amount meant desorption of dyes adsorbed in the previous process from TiO_2 to dye solution above the pH value of 3 in the following adsorption process. Desorption occurred at each pH value in the fourth adsorption process, of which data was not listed herein. The dye molecules were repelled almost completely from the surface of nanoparticles when pH value was greater than 6 in the repeated adsorption processes. After the first adsorption,

the zeta-potential values cannot reflect the electric charges of TiO_2 surface due to retained dye molecules on TiO_2 and desorbed dye molecules in water. The similar dye ionization in both adsorbed TiO_2 and water resulted in the same zeta potential at all pH values. TiO_2 did not actually reach the maximum adsorption amount and was not completely covered by dye molecules after the first adsorption. There was still electrostatic interaction for dye adsorption at the pH value of 2. As pH value increased in the following adsorption processes, dye molecules were inclined to desorb from TiO_2 surface to form dye aggregates due to decreased dye solubility. The desorption was also attributed to introduction of negative ions of the anionic dye onto the surface of nanoparticles and possible decreased surface area occupied by adsorbed dyes in the former adsorption process.

Effect of Dye Concentration on Dye Adsorption onto TiO_2

Figure 3 demonstrated the effect of dye concentration on dye adsorption amount on TiO_2 nanoparticles and dye uptake rate of dye aqueous solution in the first adsorption process. The adsorption amount increased sharply with the initial dye concentration increasing below 1 g/*l* and reached a steady state with further increment of dye concentration. Dye uptake rate above 90 % was achieved when dye concentration was lower than 1 g/*l*, implying high efficiency of dye adsorption from dye aqueous solution.

The adsorption isotherm was simulated with Langmuir and Freundlich equations. The parameters of isotherms were listed in Table 2. The higher correlation coefficient of Langmuir model (R^2=0.994, Figure 4) than Freundlich model (R^2=0.786, Figure 6) illustrated that the adsorption of the anionic dye molecules on TiO_2 nanoparticles was well described by Langmuir model, which suggested that electrostatic interaction dominated in anionic dye adsorption onto TiO_2 nanoparticles at pH value of 2 [9,22]. Nevertheless, when transformed into Scatchard equation, the adsorption data did not follow the Langmuir isotherm well (R^2=0.892). Figure 5 showed that dye partition coefficient q_e/C_e rarely changed at high concentrations of dye in the adsorbent. This could be attributed to aggregation of dye on titanium dioxide at high concentrations. However, at lower dye concentrations than 1.2 g/*l* the Langmuir model was closely fitted. The relationship between adsorption amount or uptake rate and dye concentration at pH value of 2 in the second adsorption

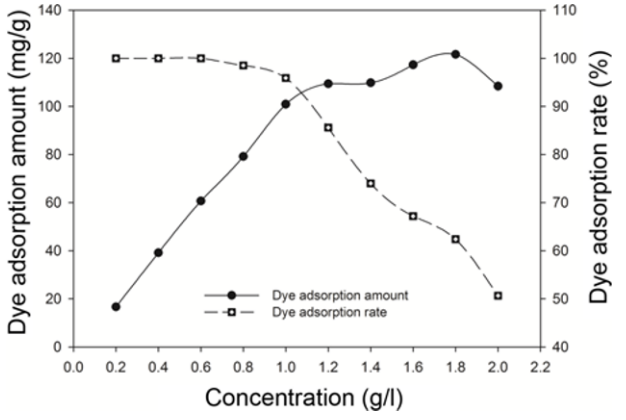

Figure 3. Effect of dye concentration on dye adsorption onto TiO_2 in the first adsorption process.

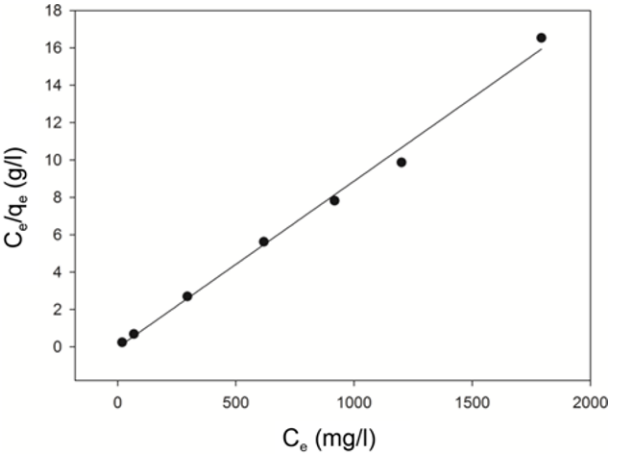

Figure 4. Fitted curve of Langmuir model.

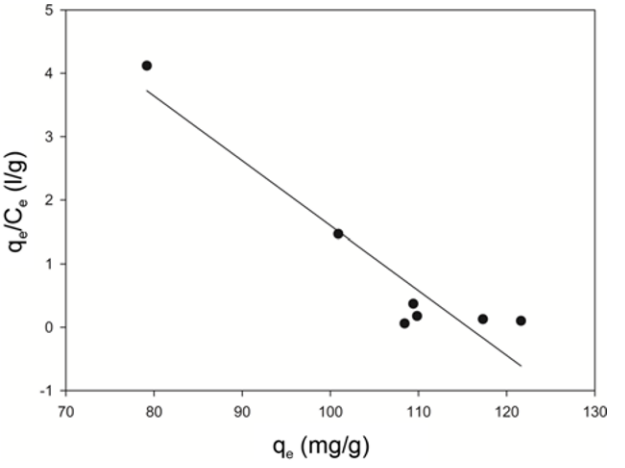

Figure 5. Fitted curve of Scatchard model.

Table 2. The parameters of different adsorption isotherm

Model		Parameter	R^2	Model		Parameter	R^2	Model		Parameter	R^2
Langmuir	K_L	-0.2242	0.994	Scatchard	q_m	115.6438 (mg/g)	0.892	Freundlich	K_F	68.2496	0.786
	q_m	112.3596 (mg/g)			K_L	0.1022			N	13.2626	

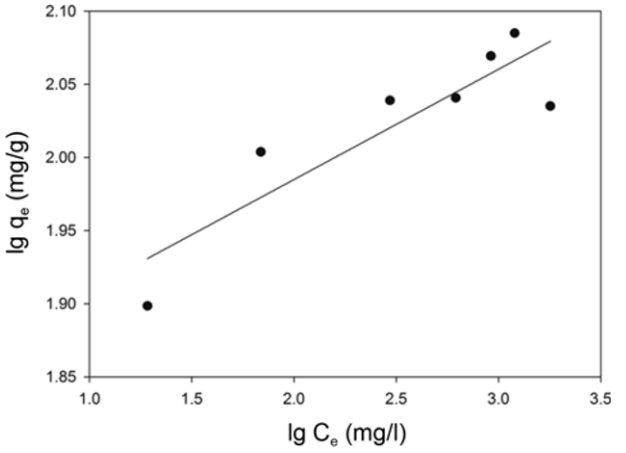

Figure 6. Fitted curve of Freundlich model.

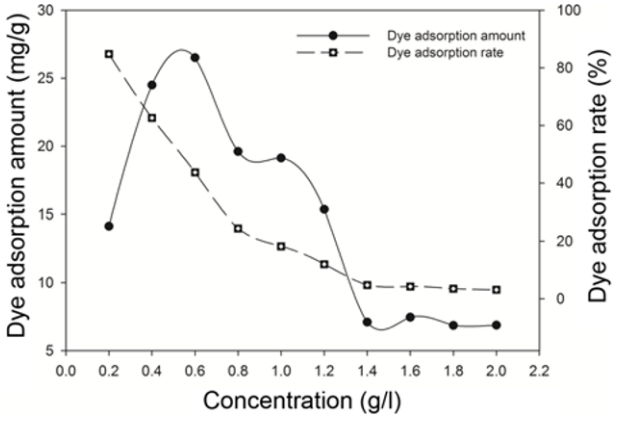

Figure 7. Effect of dye concentration on dye adsorption onto TiO_2 in the second adsorption process.

process was displayed in Figure 7. The increasing tendency below 0.6 g/*l* and decreasing tendency from 0.6 g/*l* to 1.4 g/*l* and no obvious change above 1.4 g/*l* were observed for adsorption amount of dyes. Dye uptake rate decreased when dye concentration increased. The electrostatic attraction from surface protonated sites and electrostatic repellency from anionic ions of adsorbed dyes co-existed on the surface of nanoparticles. As seen in Figure 2, zeta potential of dye adsorbed TiO_2 particles decreased even at pH value of 2 comparing with pristine TiO_2, implying decreasing protonated sits and increasing anionic sites due to introduction of the anionic dye molecules in the first adsorption process. Self-association of dye molecules formed dye aggregates of different size in dye solution. At low dye concentrations, single dye molecules and small dye aggregates were easily attracted onto protonated sites of nanoparticles. Large dye aggregates at high dye concentrations were inclined to be repelled by anionic ions of adsorbed dye molecules.

The dye desorption ratio of silane modified pigment and unmodified pigment was 4.26 % and 7.86 %, respectively.

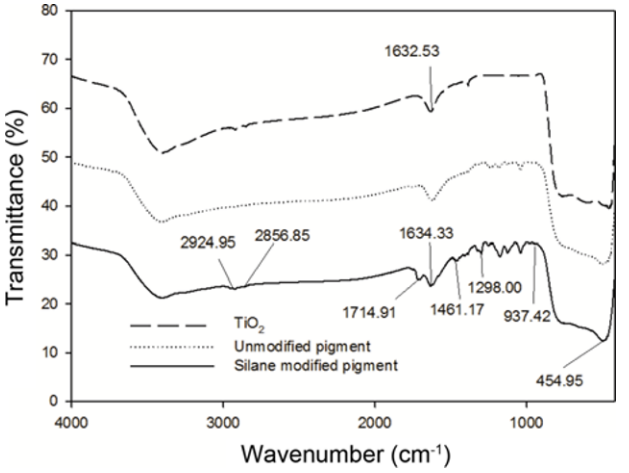

Figure 8. FT-IR spectra of TiO_2, unmodified pigment, and silane modified pigment.

The lower desorption ratio of silane modified pigment than unmodified pigment implied that the condensed film of silane polymer was capable to fixate dyes to TiO_2 surface and prevent dye desorption from TiO_2 surface during washing to some extent. Therefore, the silane coupling agent acted as fixation agent to some extent.

Structure Analysis of Pigments

The FT-IR spectra of TiO_2, dye adsorbed TiO_2 unmodified pigment, and silane modified pigment were shown in Figure 8. The peaks at 454.95 cm^{-1} and 1632.53 cm^{-1} were associated with Ti-O and Ti-OH stretching vibration [23]. The peak at 2924.95 cm^{-1} corresponded to a C-H stretching vibration of $-CH_3$ and $-CH_2$ group. The band at 1714.91 cm^{-1} was assigned to the C=O stretching vibration. The adsorption peak of C-H bending vibration and C-O symmetric stretching in acyloxy group located at 1461.17 cm^{-1} and 1289 cm^{-1}, respectively. Comparing with original TiO_2 and unmodified pigment, new peaks of silane modified pigment at 2924.95 cm^{-1}, 1714.91 cm^{-1}, 1461.17 cm^{-1}, and 1289 cm^{-1} illustrated that silane network polymer was condensed onto the surface of pigments. The weak peak at 937.42 cm^{-1} implied the possible Ti-O-Si bond [5,11].

Decoloration of Pigments

Figure 9 displayed that ΔE^* values of pigments decreased with UV irradiation time extending under UV irradiation of 254 nm and 185 nm. The color nearly vanished at 8 h, implying that dye molecules were nearly photodegraded and the decoloration of pigment was feasible under the ultraviolet with wavelength of 185 nm and 254 nm. The dye molecules could also be decomposed under 365 nm UV light to some degree. UV irradiation with wavelength less than 387 nm in the sunlight (occupying 5 % of the solar spectrum) may cause limited decoloration, which will be restrained by

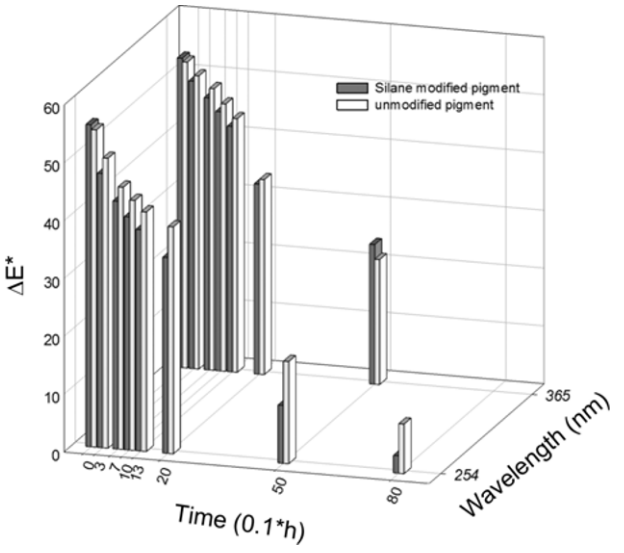

Figure 9. Decoloration of pigments under UV irradiation.

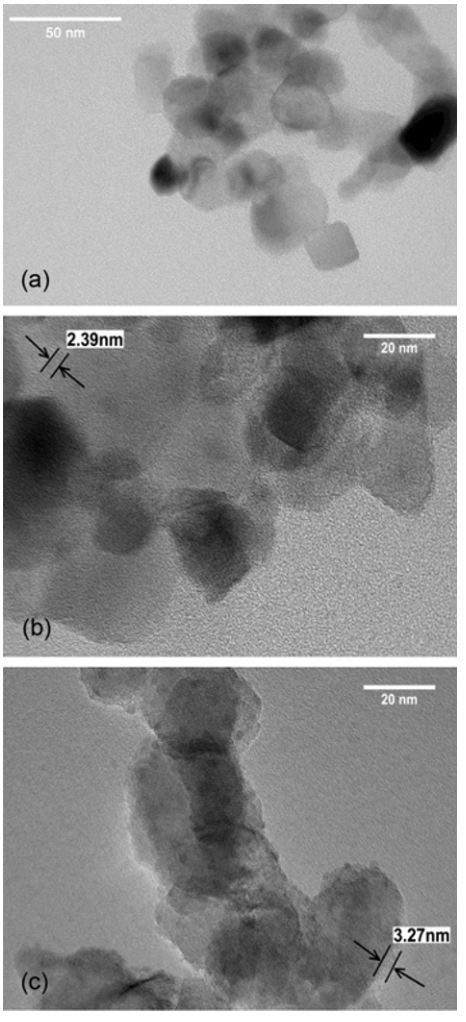

Figure 10. TEM pictures of TiO_2 (a), unmodified pigment (b), and silane modified pigment (c).

addition of UVA & UVB resistant agent at the stage of pigment modification or immobilization of pigment onto substrates. In addition, there was an interesting phenomenon that smaller ΔE^* values were found for silane modified pigments after UV irradiation comparing with unmodified pigments. The above-mentioned fitted Langmuir isotherm model suggested monolayer of dye molecules adsorbed onto TiO_2 surface due to electrostatic interaction between $TiOH_2^+$ sites and sulfonic groups of the anionic dye. A single dye molecule could be anchored longitudinally on TiO_2 surface via one sulfonic group or aligned with TiO_2 surface via two or more sulfonic groups. It was observed in Figure 10 that the thickness of adsorbed dye layer was about ~2.39 nm, corresponding to the longitudinal size of single dye molecule, which indicated possible longitudinal adsorption mode of some dye molecules. After silane modification, the silane polymer layer was attached to the surface of TiO_2 particle. The thickness of coating layer of dyes and silane polymer was about ~3.27 nm. Wu *et al.* claimed that a coating layer with the thickness of ~3.1 nm existed on neat TiO_2 particle surface after KH570 modification [5]. The thickness with slight increment indicated that the initial longitudinally adsorbed dye molecules might be aligned with the TiO_2 surface tightly due to the attached silane polymer layer. The change of adsorption mode and increasing contact area of dyes onto TiO_2 surface after silane modification might account for more efficient photodegradation of dye molecules and lighter color depth.

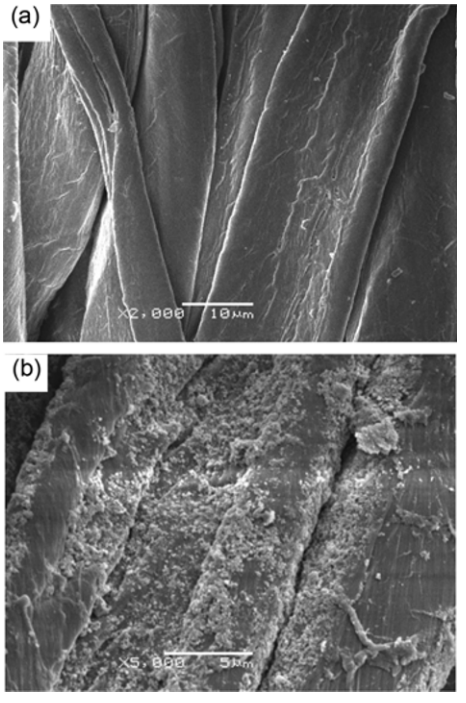

Figure 11. SEM images: (a) pristine cotton fabric and (b) pigment dyed cotton fabric with dye-fixing agent.

Table 3. Color depth and color fastness of pigment dyed fabrics

Sample	ΔE^*	*K/S*	Color fastness to rubbing (dry)	Color fastness to rubbing (wet)
Fabric with unmodified pigment	24.50	0.247	3	2-3
Fabric with silane modified pigment	25.10	0.258	4-5	3-4

Coloration and Decoloration of Cotton Fabrics with Pigments

The morphology of the pigments on the cotton fabric was shown in Figure 11. Smooth surface of pristine cotton cellulose fibers was seen. Although some aggregation was observed, the pigments with the diameter of about 200-300 nm were well distributed on the surface of cotton fabric. When the pigment was immobilized onto substrates via the film of fixation agent, the silane polymer layer on the surface of modified pigments could improve interface compatibility and double bonds in the silane layer could react with the reactive groups of fixation agent, imparting higher color depth and better rubbing fastness in Table 3.

The variation of ΔE^* after decoloration of pigment dyed fabrics under UV irradiation was seen in Figure 12. Little variation of ΔE^* was found for dyed cotton fabric without UV absorber under UV irradiation at the wavelength of 365 nm and dyed cotton fabrics treated with UV absorber at both 365 nm and 185 & 254 nm. The color depth decreased by 40.3 % without UV absorber at 185 & 254 nm. Fortunately, no UVC light with the wavelength of less than 280 nm reached the earth due to the light absorption of ozonosphere. Moreover, UVA an UVB in the range of 280-400 nm occupies approximately 5 % of the solar irradiation.

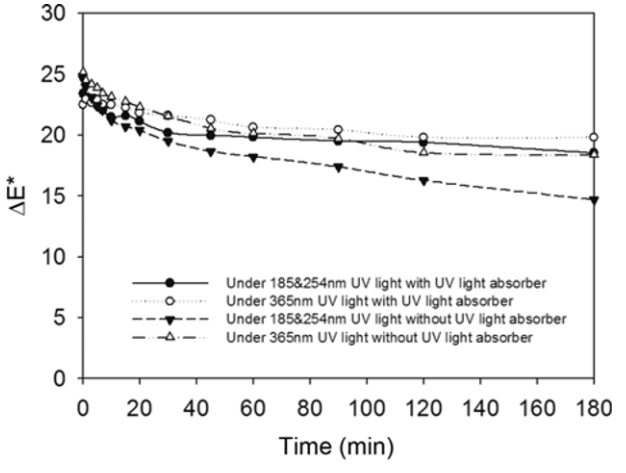

Figure 12. The variation of ΔE^* after decoloration of dyed fabrics under UV irradiation.

Thus, the TiO_2 composite pigment was safe in the normal life cycle, especially with the UV resistant agent blocking UV radiation in the sunlight.

Conclusion

The dye enwrapped TiO_2 composite pigments with different color depth could be obtained through adjusting pH values and adsorption times and varying dye concentration of dye aqueous solution. Silane modification after dye adsorption onto TiO_2 surface was conducive to dye fixation in the pigment, immobilization of pigment onto substrates and more efficient photodegradation of dye molecules. Good dyeability and color fastness to rubbing was obtained. The TiO_2 composite pigment was safely to use in the normal life cycle of textiles, especially with the UV resistant agent blocking UV radiation in the sunlight. The decoloration of pigment was achieved via photodegradation of dye molecules by radicals produced from photoexcited TiO_2 particles under specific UV treatment with short wavelength.

Acknowledgement

This work was financially supported by Cultivation Program for Dalian Excellent Talents of Science and Technology (No.2015R082).

References

1. K. Nakata and A. Fujishima, *J. Photochem. Photobiol. C*, **13**, 169 (2012).
2. N. M. Mahmoodi, *Desalination*, **279**, 332 (2014).
3. H. X. Guo, K. L. Lin, Z. S. Zheng, F. B. Xiao, and S. X. Li, *Dyes Pigm.*, **92**, 1278 (2012).
4. E. Stathatos, D. Papoulis, C. A. Aggelopoulos, D. Panagiotaras, and A. Nikolopoulou, *J. Hazard. Mater.*, **211-212**, 68 (2012).
5. W. S. Ni, S. P. Wu, and Q. Ren, *Chem. Eng. J.*, **214**, 272 (2013).
6. B. Ohtani, *J. Photochem. Photobiol. C.*, **11**, 157 (2010).
7. T. Jesionowski, A. Przybylska, B. Kurc, and F. Ciesielczyk, *Dyes Pigm.*, **89**, 127 (2011).
8. J. Xia and S. Yanagida, *Sol. Energy*, **85**, 3143 (2009).
9. W. Wu, G. L. Zhao, and G. R. Han, *Rare Metal Mater. Eng.*, **37**, 167 (2008).
10. M. Janus and A. W. Morawski, *Appl. Catal. B*, **75**, 118 (2007).
11. I. H. Cho and K. D. Zoh, *Dyes. Pigm.*, **75**, 533 (2007).
12. K. Siwińska-Stefańska, M. Nowacka, A. Kolodziejczak-Radzimska, and T. Jesionowski, *Dyes. Pigm.*, **94**, 338 (2012).
13. J. Zhao, M. Milanova, M. C. G. M. Warmoeskerken, and V. Dutschk, *Colloids Surf. A*, **413**, 273 (2012).
14. R. Tomovska, V. Daniloska, and M. J. Asua, *Appl. Surf.*

Sci., **264**, 670 (2013).
15. T. Jesionowski, A. Przybylska, B. Kurc, and F. Ciesielczyk, *Dyes Pigm.*, **88**, 116 (2011).
16. C. Y. K. Lung and J. P. Matinlinna, *Dent. Mater.*, **28**, 467 (2012).
17. J. Du, L. Zhang, and S. Chen, *Color. Technol.*, **121**, 29 (2005).
18. M. Luo, X. Zhang, and S. Chen, *Color. Technol.*, **119**, 297 (2003).
19. H. Granbohm, K. Kulmala, A. Iyer, Y. Ge, and S. P. Hannula, *Water Air Soil Pollut.*, **228**, 127 (2017).
20. N. Kannan and M. M. Sundaram, *Dyes. Pigm.*, **51**, 25 (2001).
21. S. Xu, Y. Gao, X. Sun, M. Yue, Q. Yue, and B. Gao, *RSC Adv.*, **6**, 101198 (2016).
22. S. H. Fan, Z. F. Sun, Q. Z. Wu, and Y. G. Li, *Acta Phys. Chim. Sin.*, **19**, 25 (2003).
23. S. Mallakpour and R. Aalizadeh, *Prog. Org. Coat.*, **76**, 648 (2013).